Conductivity imaging by the method of characteristics in the 1-Laplacian

Alexandru Tamasan† and Johann Veras‡

†‡Department of Mathematics, University of Central Florida, Orlando, FL, USA

E-mail: †tamasan@math.ucf.edu, ‡jveras@knights.ucf.edu

Abstract. We consider the problem of reconstruction of a sufficiently smooth planar conductivity from the knowledge of the magnitude $|J|$ of one current density field inside the domain, and the corresponding voltage and current on a part of the boundary. Mathematically, we are lead to the Cauchy problem for the the 1-Laplacian with partial data. Different from existing works, we show that the equipotential lines are characteristics in a first order quasilinear partial differential equation. The conductivity can be recovered in the region flown by the characteristics originating at parts of the boundary where the data is available. Numerical experiments show the feasibility of this alternative method.

1. Introduction

In this paper we present a novel reconstruction method in Current Density based Impedance Imaging (CDII): Let $\Omega \subset \mathbf{R}^2$ be a simply connected, bounded domain with piecewise smooth boundary, and σ be a sufficiently smooth conductivity in Ω bounded away from zero and infinity. A current g with $\int_{\partial\Omega} g ds = 0$ is normally injected at the boundary. Up to an additive constant, the voltage potential u distributes according to the solution of the Neumann problem

$$\nabla \cdot \sigma \nabla u = 0, \qquad \sigma \partial_\nu u|_{\partial\Omega} = g, \tag{1}$$

where ν is the outer unit normal to the boundary. The current density field J is uniquely defined by Ohm's law $J = -\sigma \nabla u$, regardless of the constant. We assume that its magnitude $|J|$ is known in Ω (or some subregion). Currently, knowledge of J inside can be obtained from a technique developed in [26] based on magnetic resonance measurements, but new techniques seek to employ acoustic measurements [28].

For clarity, we convene that properties referring to a boundary arc concern only the interior points. Properties pertaining to its end points are to be specified separately. We assume that the voltage u is measured on a boundary arc Γ on which the non-stationary condition

$$|\partial_\tau (u|_\Gamma)| > 0 \tag{2}$$

holds, where τ is the unit tangent. At a corner point both sided tangential derivatives are to satisfy (2). At the end points $\partial_\tau u|_\Gamma$ (or one sided derivative if it is a corner point) may vanish.

The CDII problem of concern here is the reconstruction of σ inside Ω from (partial) knowledge of $|J|$ inside, and the values of f, and g along Γ. This problem belongs to the recently developed class of imaging methods from dual physics. Among the works which considered interior knowledge of current density for conductivity imaging we mention [29], [14], [15], [16], [13], [17], [25] and references below; see [24] for a survey on Current Density Imaging from minimal data. In [19] and [18] the interior knowledge of one component of the magnetic field is employed; see [27] for comprehensive references in this direction. Recent works for conductivity imaging from dual physics consider some electro-acoustic or magneto-acoustic measurements, see [20], [5],[4], [10], and [6].

By taking the absolute value in Ohm's law and plugging it into the conductivity equation in (1), the conductivity imaging problem becomes the Cauchy problem for the 1-Laplacian (in the metric $|J|^2 ds$):

$$\nabla \cdot \frac{|J|}{|\nabla u|} \nabla u = 0, \quad u|_\Gamma = f, \quad \partial_\nu u|_\Gamma = g, \tag{3}$$

where ν is the outer unit normal to the boundary.

The work [14] is the first to employ the 1-Laplacian in conductivity imaging in conjunction with Neumann boundary conditions. As shown in there, the Neumann problem can have none to multiple solutions, to conclude that one current density field by itself, in general, cannot determine the conductivity inside. To remedy this, in [21]

the Cauchy problem (3) is considered and sufficient conditions on the boundary voltage are found to recover the conductivity stably. Further work in [22] and [25] consider the Dirichlet problem for the 1-Laplacian to show that boundary voltage on the entire boundary together with $|J|$ inside uniquely determine σ (this is in any dimension $d \geq 2$). In two dimensions the result is extended to imaging from partial data [23].

A marked difference from the approach in [21] is that in here one first injects a current, rather than maintain a specific voltage. As in [14], the current g satisfies

$$g|_{\Gamma_+} > 0, g|_{\Gamma_-} < 0, \text{ and, } g|_{\partial\Omega\setminus\Gamma_\pm} = 0, \tag{4}$$

where $\Gamma_\pm$ are two connected arcs. This applied current pattern is important since it yields

$$\inf_{\overline{\Omega}} |\nabla u| > 0, \tag{5}$$

see [2, 3].

Throughout the paper $C^{k,\alpha}(\Omega)$, $\alpha \in (0,1)$, denotes the space of differentiable functions with α-Hölder continuous k-th derivative, for some $0 < \alpha < 1$. If $\alpha = 1$ then the k-th derivative is assumed Lipschitz. The conductivity reconstruction is based on the following local existence and uniqueness result.

Theorem 1.1 *Let $\Omega \subset \mathbf{R}^2$ be a domain with piecewise Lipschitz boundary, and Γ be a smooth boundary arc. Assume that $|J| \in C^{1,1}(\Omega \cup \Gamma)$ is positive in a neighborhood of Γ. Let $g \in C^1(\Gamma)$, and $f \in C^2(\Gamma)$ be such that*

$$|f_\tau| > 0, \quad \textit{inside} \quad \Gamma, \tag{6}$$

where f_τ denotes the tangential derivative. Then there is a neighborhood $\tilde{\Omega}$ of Γ, in which (3) has a unique solution $u \in C^1(\tilde{\Omega})$ with $|\nabla u| \neq 0$.

Assume that $|J|$ is known in a sub-domain $\tilde{\Omega} \subset \Omega$ adjacent to Γ. Then the conductivity can be determined in a part of the domain as described by the result below.

Theorem 1.2 *Let $\Omega \subset \mathbf{R}^2$ be a simply connected domain with piecewise $C^{3,\alpha}$-smooth boundary, $\sigma \in C^{2,\alpha}(\Omega)$ be a smoothly varying conductivity with unknown values inside Ω but known boundary values. A current $g \in C^{1,\alpha}(\partial\Omega)$ satisfying (4) is applied at the boundary, and the voltage potential $u|_\Gamma$ is measured along a boundary arc Γ to satisfy (2). Assume that the magnitude of the current density field $|J|$ generated by the injected current is known in a subdomain $\tilde{\Omega} \subset \Omega$ with $\Gamma \cap \partial\tilde{\Omega} \neq \emptyset$. Then the conductivity can be uniquely recovered in the region spanned by the characteristics that originate on $\Gamma \cap \partial\tilde{\Omega}$ and stay within $\tilde{\Omega}$.*

Different from the method in [21], we show that the voltage potential u is constant along the characteristics of a quasilinear first order differential equation, see (9) below. As a direct consequence of the smooth dependence on the data (see, e.g., [12]) of solutions of initial value problems for systems of ordinary differential equations (ODE's), we show that the method is conditionally stable in a compact subset of the region flown by the characteristics.

Theorem 1.3 (Conditional Stability) *Let $\Omega \subset \mathbf{R}^2$ be a simply connected domain with piecewise $C^{3,\alpha}$-smooth boundary, and $\sigma \in C^{2,\alpha}(\Omega)$ be an unknown conductivity. Let u be the solution of (1) for some applied current g satisfying (4), Γ be an arc at the boundary such that (2) holds on $\overline{\Gamma}$, and $|J| := \sigma|\nabla u|$ be known in Ω. Assume that $\tilde{g} \in C^1(\partial\Omega)$, $\tilde{f} \in C^2(\Gamma)$, and $|\tilde{J}| \in C^{1,1}(\overline{\Omega})$ are "noisy data" such that*

$$\max\{\|\partial_\tau(u|_\Gamma) - \tilde{f}_\tau\|_{C^1(\Gamma)}, \|g - \tilde{g}\|_{C^1(\partial\Omega)}, \|\nabla \ln|J| - \nabla \ln|\tilde{J}|\ \|_{Lip(\overline{\Omega})}\} \leq \eta, \quad (7)$$

for some $\eta > 0$ small enough. Let $\tilde{u}$ be defined along the characteristics for the noisy data $\tilde{g}, \tilde{f}, |\tilde{J}|$ as in (16). Let $\Omega_\Gamma \subset \Omega$ be the intersection of the domains spanned by characteristics originating at $\overline{\Gamma}$ for the two sets of data. Then, at each point in Ω_Γ

$$\left|\sigma - \frac{|\tilde{J}|}{|\nabla \tilde{u}|}\right| \leq \omega(\eta),$$

for some map $\omega : [0, \epsilon) \to [0, \infty)$ with $\omega(\eta) \to 0$ as $\eta \to 0$, which depends on $\|\nabla \ln|J|\|_{Lip(\overline{\Omega})}$, $\|g\|_{C^1(\Gamma)}$, $\|f|_\Gamma\|_{C^2(\Gamma)}$, and the modulus of continuity of σ.

The reconstruction methods described in the proof of the theorems above are implemented in Section 3. Complete and incomplete interior data results are presented. The algorithms are based on the numerical solutions of the Cauchy problem for the characteristic system and the spline interpolation.

2. The method of reconstruction

In this section we prove Theorems 1.1, 1.2, and 1.3.

Proof of Theorem 1.1: We first assume existence and address the local uniqueness question. Let $u_i \in C^1(\Omega_i \cup \Gamma)$, $i = 1, 2$, be two solutions of (3) defined nearby Γ such that $|\nabla u_i| > 0$. Let $s \mapsto (x_0(s), y_0(s))$ be the Euclidean arc-length parametrization of Γ. The assumption (2) yields

$$f_\tau(x_0(s), y_0(s)) := \langle x_0'(s), y_0'(s)\rangle \cdot \nabla u_i(x_0(s), y_0(s)) \neq 0, \quad i = 1, 2. \quad (8)$$

Since $|\nabla u_i| \neq 0$ in $\Omega_1 \cap \Omega_2$, which is a simple connected neighborhood of Γ, the argument functions $\theta_i = \arg(\nabla u_i)$ are $C^1(\Omega_1 \cap \Omega_2)$-smoothly defined for $i = 1, 2$. Since u_i are solutions of the 1-Laplacian in (3), it is easy to see that they satisfy

$$-(\sin\theta)\theta_x + (\cos\theta)\theta_y + (\ln|J|)_x \cos\theta + (\ln|J|)_y \sin\theta = 0. \quad (9)$$

To simplify notation in what follows we let

$$\theta_0(s) := \arg(f_\tau \partial_\tau + g\partial_\nu)|_{(x_0(s), y_0(s))}, \quad (10)$$

where $\{\partial_\tau, \partial_\nu\}$ is the positively oriented orthonormal frame of the unit tangent and normal vector on Γ.

Now let $t \mapsto (x_i(t, s), y_i(t, s))$ be the (Euclidean arc-length) parametrization of the equipotential maps $u_i(x_i(t, s), y_i(t, s)) = f(s)$, $i = 1, 2$. Then the map $t \mapsto (x_i(t, s), y_i(t, s), \theta_i(t, s))$ solves the corresponding characteristic system

$$\begin{cases} \frac{dx}{dt} = -\sin\theta \\ \frac{dy}{dt} = \cos\theta \\ \frac{d\theta}{dt} = -(\ln|J|)_x \cos\theta - (\ln|J|)_y \sin\theta, \end{cases} \quad (11)$$

subject to the initial conditions

$$x(0,s) = x_0(s), \quad y(0,s) = y_0(s), \quad \theta(0,s) = \theta_0(s), \tag{12}$$

where θ_0 defined in (10).

Uniqueness in the initial values problem for ODE implies that $(x_1(t,s), y_1(t,s)) = (x_2(t,s), y_2(t,s))$ whenever $(x_i(t,s), y_i(t,s)) \in \Omega_1 \cap \Omega_2$. Therefore u_1 and u_2 are constant on each other level sets. Since they also coincide at $t = 0$, they coincide in the region spanned by the family of curves $t \mapsto (x_1(t,s), y_1(t,s))$, $0 < s < Length(\Gamma)$.

The necessary and sufficient condition for an arbitrary curve $\gamma : s \mapsto (x_0(s), y_0(s))$ to be non-characteristic for (9) is for the determinant

$$\left| \begin{array}{cc} -\sin\theta_0(s) & x_0'(s) \\ \cos\theta_0(s) & y_0'(s) \end{array} \right| \neq 0. \tag{13}$$

By the hypothesis (8), the curve Γ is non-characteristic for the equation (9), and the pair (s,t) defines local coordinates near Γ, which yield that $u_1 = u_2$ in an open neighborhood of Γ. A monodromy argument extends the region of uniqueness to a maximal, simply connected set, see also (15).

To prove the local existence for solutions to the Cauchy problem (3) consider the problem (11) subject to the initial conditions

$$x(0,s) = x_0(s), \quad y(0,s) = y_0(s), \quad \theta(0,s) = \theta_0(s), \tag{14}$$

where $s \mapsto (x_0(s), y_0(s))$ is the arc-length parametrization of Γ, and $\theta_0(s)$ is defined in (10).

The hypothesis $f_\tau > 0$ at Γ together with the smoothness assumptions on the boundary data yields a C^1-smoothly defined argument map $\arg(f_\tau \partial_\tau + g\partial_\nu)$ along Γ. Since the right hand side of (11) is Lipschitz, for each s there exists a unique solution $t \mapsto (x(t,s), y(t,s), \theta(t,s))$ with t in some interval $[0, \beta(s))$. Moreover, since the initial conditions are C^1-smooth in parameter s, the solutions are also C^1 in the parameter s (they are already $C^{1,1}$ in t), see [12]. Define the sub-domain

$$\Omega_0 := \{(x(t,s), y(t,s)) \in \tilde{\Omega} : s \in (0, length(\Gamma)), t \in (0, \beta(s))\}, \tag{15}$$

the function u in Ω_0 by

$$u(x(t,s), y(t,s)) := f(x_0(s), y_0(s)), \tag{16}$$

and the discriminant

$$\Delta(t,s) := \left| \begin{array}{cc} -\sin\theta(t,s) & x_s(t,s) \\ \cos\theta(t,s) & y_s(t,s) \end{array} \right| = \left| \begin{array}{cc} x_t(t,s) & x_s(t,s) \\ y_t(t,s) & y_s(t,s) \end{array} \right|. \tag{17}$$

Since Γ is non-characteristic at every point, the equation (13) yields $\Delta(0,s) \neq 0$, for all $s \in (0, Length(\Gamma))$. Continuity of Δ implies that

$$\Delta(t,s) \neq 0, \quad \text{in} \quad \{(s,t) : \ s \in (0, length(\Gamma)), \ t \in [0, \tilde{\beta}(s))\},$$

for some $\tilde{\beta}(s) \leq \beta(s)$. Let us define

$$\Omega_1 := \{(x(s,t), y(t,s)) \in \Omega_0 : \ \Delta(t,s) \neq 0\}. \tag{18}$$

By differentiating in t and s (16) we get that

$$\nabla u(x(s,t),y(s,t)) = -\frac{f_\tau(x_0(s),y_0(s))}{\Delta(t,s)}\langle \cos\theta(t,s), \sin\theta(t,s)\rangle. \tag{19}$$

In particular

$$\frac{\nabla u(x,y)}{|\nabla u(x,y)|} = \langle \cos\theta(x,y), \sin\theta(x,y)\rangle, \quad (x,y)\in\tilde{\Omega}.$$

Since θ solves (9) then u solves the 1-Laplacian in Ω_1. A rotation of coordinates gives that $\partial_\nu u = g$ at Γ. □

Note that the formula (13) says that the tangent at the boundary must not to be perpendicular to the $\nabla u(\gamma(s))$, or that the tangent must be transversal to the equipotential line of u at the point $(x_0(s), y_0(s))$.

Proof of Theorem 1.2: Since u solves the Cauchy (3), it remains to show that our assumptions are sufficient to yield $\nabla \ln|J| \in Lip(\Omega)$. Indeed, since the boundary $\partial\Omega$ is piecewise $C^{2,\alpha}$, $\sigma \in C^{2,\alpha}(\Omega)$, and $g \in C^{1,\alpha}(\partial\Omega)$ by the elliptic regularity (see e.g. [11]) of solutions o (1) yields $u \in C^{3,\alpha}(\overline{\Omega})$. Consequently, we obtain $|J| \in C^{2,\alpha}(\overline{\Omega})$. Moreover, since σ is bounded away from zero, and no singularities present due to the choice of the applied current, we also obtain $\min_{\overline{\Omega}}|J| > 0$. Therefore $\nabla \ln|J| \in C^{1,\alpha}(\overline{\Omega}) \subset Lip(\Omega)$. □

The absence of singular points as in (5) makes the result [21, Lemma 3.1] still valid: Each equipotential set is a smooth curve of finite length and with the two endpoints at the boundary. In particular each point inside lies on a unique equipotential line which reaches the boundary. If $|J|$ is known in the entire domain Ω, then (by the uniqueness of solution in the initial value problem for ODEs,) the method recovers the entire equipotential line originating at Γ.

Proof of Theorem 1.3: In the followings, we distinguish the quantities corresponding to the "noisy data" $(\tilde{g}, \tilde{J}, \tilde{f})$, by using a tilde $(\tilde{\cdot})$ in their notation. For example $\tilde{\Delta}$ denotes the discriminant in (17) corresponding to the noisy data.

Note that $\tilde{g}$ need not satisfy the pattern in (4). Instead by choosing η in (7) such that

$$0 < \eta < \min\{\min_{\Gamma}(f_\tau), \min_{\overline{\Omega}}|\nabla \ln|J||\}$$

we obtain $\tilde{f}_\tau > 0$ on Γ, and $|\tilde{J}| > 0$ in $\overline{\Omega}$. In particular $\ln|\tilde{J}| \in C^{1,1}(\Omega)$, which suffices to solve locally the Cauchy problem (3) associated with $\tilde{g}$ on $\partial\Omega$, $\tilde{f} \in \Gamma$, and $|\tilde{J}|$ in Ω. More precisely, the initial problem (11) and (12) yields a solution $t \mapsto (\tilde{x}(t,s), \tilde{y}(t,s), \tilde{\theta}(t,s))$, for each $s \in (0, Length(\Gamma))$ and $t \in (0, \tilde{\beta}(s))$. Here $\tilde{\beta}(s)$ represents the Euclidean length of the characteristic originating at the point $(x_0(s), y_0(s)) \in \Gamma$.

We estimate the error at

$$(x^*, y^*) := (x(t,s), y(t,s)) = (\tilde{x}(\tilde{t},\tilde{s}), \tilde{y}(\tilde{t},\tilde{s})),$$

an arbitrary point in Ω_Γ. To simplify notations, we refer to a point in Ω_Γ in the coordinates defined by the characteristics. For example

$$|J|(t,s) := |J|(x(t,s),y(t,s)), \quad |J|(\tilde{t},s) := |J|(\tilde{x}(\tilde{t},s),\tilde{y}(\tilde{t},\tilde{s})),$$
$$|\nabla u|(t,s) := |\nabla u|(x(t,s),y(t,s)), \quad |\nabla \tilde{u}|(\tilde{t},\tilde{s}) := |\nabla \tilde{u}|(\tilde{x}(\tilde{t},\tilde{s}),\tilde{y}(\tilde{t},\tilde{s})).$$

Using the definition in (19) we get

$$\left|\sigma(t,s) - \frac{|\tilde{J}|}{|\nabla\tilde{u}|}(\tilde{t},\tilde{s})\right| \leq |\sigma(t,s) - \sigma(\tilde{t},\tilde{s})| + \left|\,|J|(t,s)\frac{|\Delta(t,s)|}{|f_\tau(s)|} - |\tilde{J}|(\tilde{t},\tilde{s})\frac{|\tilde{\Delta}(\tilde{t},\tilde{s})|}{|\tilde{f}_\tau(\tilde{s})|}\right|. \tag{20}$$

The continuous dependence on the data of solutions of ODE's bounds the first term in the right hand side of (20) by some modulus of continuity $\omega(\eta)$ which depends on σ. By triangle inequality it can be easily seen that the second term in the right hand side of (20) is bounded by

$$\frac{|J|}{|f_\tau|}\left|\Delta - \tilde{\Delta}\right| + \frac{|J||\tilde{\Delta}|}{|f_\tau\tilde{f}_\tau|}\left|\tilde{f}_\tau - f_\tau\right| + \frac{|\tilde{\Delta}|}{|\tilde{f}_\tau|}\left||J| - |\tilde{J}|\right|, \tag{21}$$

where for brevity we dropped the arguments, but they are still as in (20). The C^1-smooth dependence on the data, yield that Δ and $\tilde{\Delta}$ defined in (17) depend continuously on $(f_\tau, g, |J|)$, respectively on $(\tilde{f}_\tau, \tilde{g}, |\tilde{J}|)$. In particular $\Delta, \tilde{\Delta}$ are bounded on compacta. Recall also that $f_\tau, \tilde{f}_\tau$ are bounded away from zero on $\overline{\Gamma}$. Using (21), we conclude that the second term of (20) is also bounded by some modulus of continuity $\omega(\eta)$. □

Since the modulus of continuity ω depends on σ, the Theorem 1.3 only shows conditional stability.

3. Numerical results

In this section we present various numerical experiments with two different types of conductivities to demonstrate the computational capabilities of the reconstruction method above.

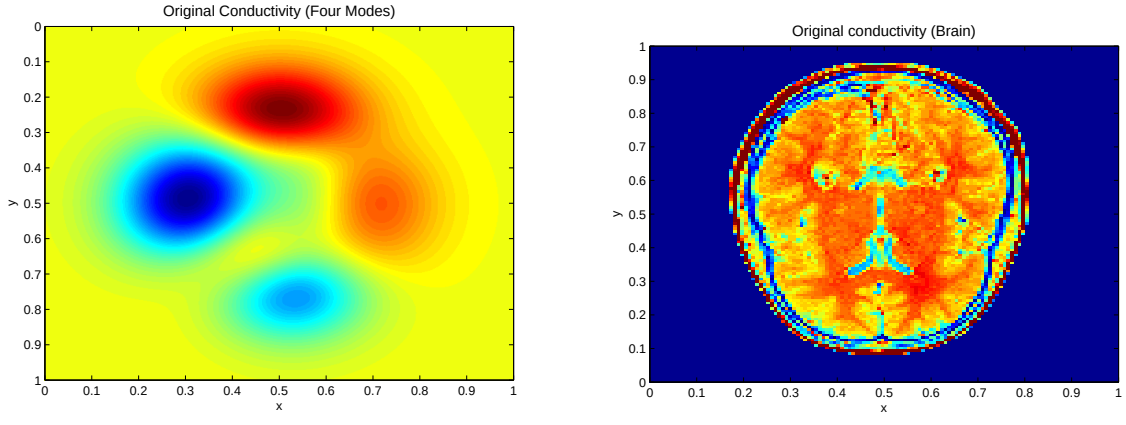

Figure 1. The original conductivity distribution map: the four modes (left) and the cross section of a human brain (right).

3.1. Data

The magnitude of the current density $|J|$ and the boundary voltage potential measurement f for the numerical experiments are obtained numerically.

We solve the Neumann problem (1) for two different conductivities by using the finite element method in MATLAB's PDE toolbox. The domain Ω is the unit box $[0,1] \times [0,1]$, and the boundary current $\tilde{g}(0,y) = \tilde{g}(1,y) = 0$, $\tilde{g}(x,1) = 1$, and $\tilde{g}(x,0) = -1$ is applied at the boundary. The first conductivity map is smoothly defined by the four modes function

$$\sigma(x,y) = 1 + 0.3 \cdot (A(x,y) - B(x,y) - C(x,y)), \tag{22}$$

where

$$\begin{aligned} A &= 0.3 \cdot [1 - 3(2x-1)]^2 \cdot e^{-9\cdot(2x-1)^2-(6y-2)^2}, \\ B &= \left[\frac{3(2x-1)}{5} - 27\cdot(2x-1)^3 - [3\cdot(2y-1)]^5\right] \cdot e^{-\left[9\cdot(2x-1)^2+9\cdot(2y-1)^2\right]}, \\ C &= e^{-[3\cdot(2x-1)+1]^2-9\cdot(2y-1)^2}; \end{aligned}$$

see the left image in Figure 1. The second conductivity is a piecewise-smooth function given by a CT image of a human brain, shown in Figure 1 on the right. The values of the pixels of the CT image are scaled to model a conductivity distribution ranging from 1 to 1.8 S/m.

The gradient of the potential ∇u is computed via differentiation of interpolating fifth degree Lagrange polynomials. The interior data $|J| = \sigma|\nabla u|$ is computed in Ω and in the sub-domain $\Omega_1 = [0, 0.6] \times [0.25, 0.701]$ for each of the aforementioned voltage potentials. Finally, the boundary voltage potentials $u|_\Gamma = f$ and $u|_{\Gamma_1} = f_1$ are measured on the arcs $\Gamma = \{0\} \times [0,1]$, and $\Gamma_1 = \{0\} \times [0.25, 0.701]$, respectively. See Figure 2 for the magnitude of the current density generated over Ω for the four modes and the brain.

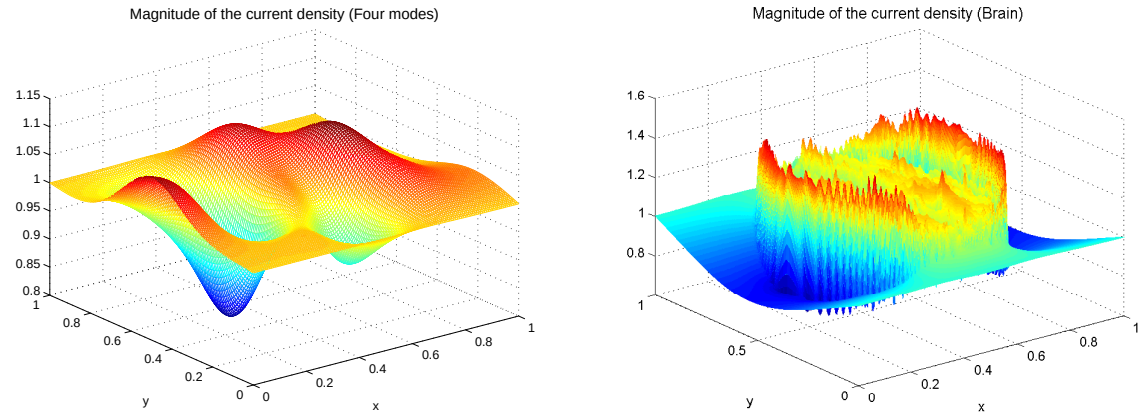

Figure 2. Magnitude of the current density of the four modes (left) and the cross section of a human brain (right) generated over the box $[0,1] \times [0,1]$.

3.2. Numerical reconstruction of the conductivity

Here we describe the steps to reconstruct a conductivity map in Ω using the method construed in section 2.

Step 1. Recall that in section 3.1 the injected current satisfies (4), hence $\theta = \frac{\pi}{2}$ on the line segment where the voltage potential is measured. Given $|J|$ in a box $[0, c] \times [a, b]$, we solve (11) using the adaptive Runge-Kutta-Fehlberg ODE solver for m characteristics subject to the initial conditions

$$x_j(0) = 0, y_j(0) = s_j, \theta_j(0) = \frac{\pi}{2}, \tag{23}$$

where $s_j = a + j\frac{b-a}{m-1}$, and $j = 1, 2, \ldots, m$.

The third equation in (11) contains the derivative of $\ln |J|$ in the direction of the unit vector $\eta = \langle \cos\theta, \sin\theta \rangle$:

$$\frac{d\theta}{dt} = -\partial_\eta \ln |J|.$$

In order to decrease the error made in differentiating $\ln |J|$ we use the center difference for the directional derivative:

$$\partial_\eta \ln |J|(x_j(t_{j_k}), y_j(t_{j_k})) = \frac{1}{2h}\left[\ln |J|(x^{j_k}_{j+h}, y^{j_k}_{j+h}) - \ln |J|(x^{j_k}_{j-h}, y^{j_k}_{j-h})\right],$$

where

$$\begin{aligned}
x^{j_k}_{j+h} &= x_j(t_{j_k}) + h \cdot \cos\theta_j(t_{j_k}),\\
x^{j_k}_{j-h} &= x_j(t_{j_k}) - h \cdot \cos\theta_j(t_{j_k}),\\
y^{j_k}_{j+h} &= y_j(t_{j_k}) + h \cdot \sin\theta_j(t_{j_k}),\\
y^{j_k}_{j-h} &= y_j(t_{j_k}) - h \cdot \sin\theta_j(t_{j_k}).
\end{aligned}$$

In all the numerical experiments the value of $\ln |J|$ (or $|J|$) at a point is interpolated by the bi-quintic piecewise Lagrange polynomials for points away from the boundary, and the bi-cubic or bi-linear interpolation for points near the boundary. For incomplete interior data, we extend $|J|$ outside the region $[0, c] \times [a, b]$ (where it is given) bi-linearly. The characteristic curves that exit this region are cut off. See, for example, the curve lying closest to the lower boundary in Figure 3.

Step 2. The characteristics are equipotential lines. The value of the potential along each characteristic is determined by the measurement of the voltage potential at the boundary. Let

$$\gamma_j(t) = (x_j(t), y_j(t)),\ j \in \{1, 2, \ldots, m\}, t \in [0, \beta_j), \tag{24}$$

denote the equipotential line, which solves (11) subject to (23), and

$$\zeta_i(\xi) = (\hat{x}_i(\xi), \hat{y}_i(\xi)), \xi \in [0, \alpha_i),\ i \in \{1, 2, \ldots, n\}, \tag{25}$$

denote a smooth non-characteristic curve, which is transversal to each $\gamma_j, j = 1, 2, \ldots, m$. At the point of intersection we have

$$\begin{cases} 0 = u_x \frac{dx_j}{dt} + u_y \frac{dy_j}{dt}, \\ u_\xi = u_x \frac{d\hat{x}_i}{d\xi} + u_y \frac{d\hat{y}_i}{d\xi}, \end{cases}$$

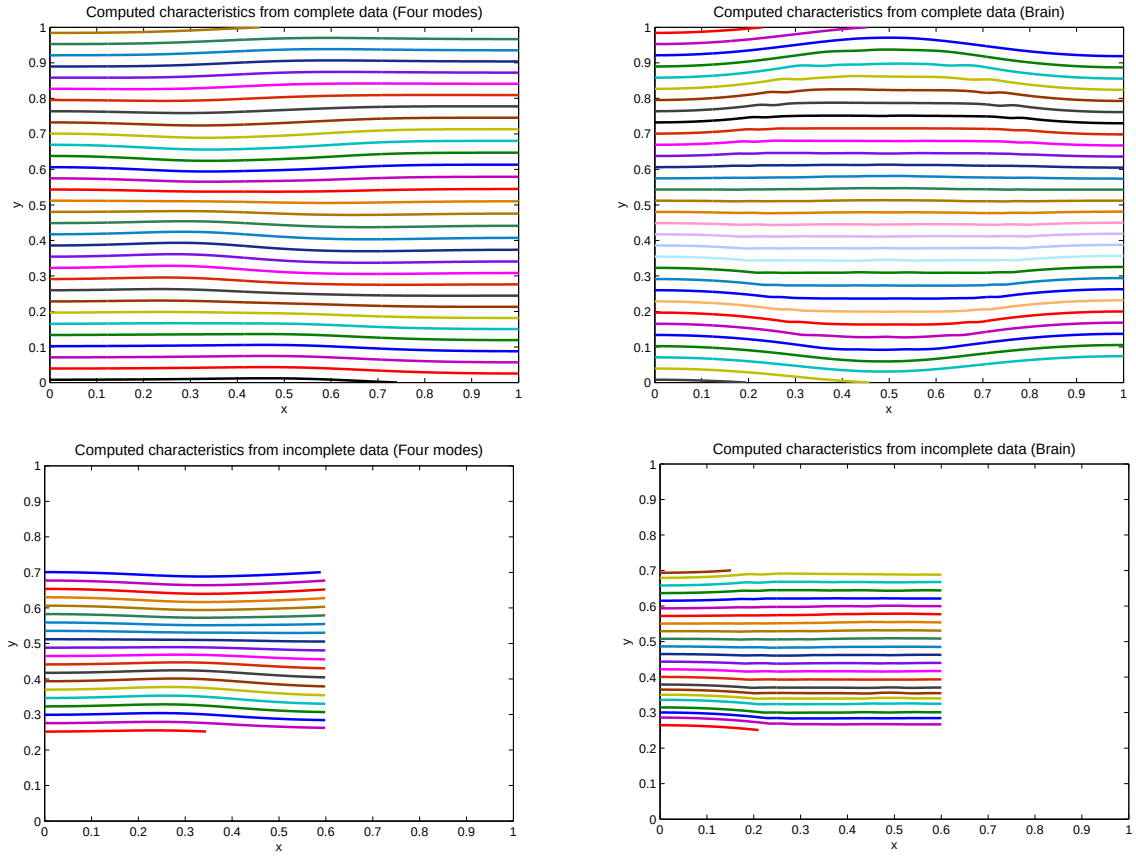

Figure 3. The top images show the characteristics of the four modes (left) and the brain (right) reconstructed from the interior data measured in $[0,1]\times[0,1]$. The bottom images show the characteristics for the four modes (left) and the brain (right) reconstructed from the interior data measured in $[0,0.6]\times[0.25,0.701]$.

and

$$\nabla u = \frac{u_\xi}{\frac{dy_j}{dt}\frac{d\hat{x}_i}{d\xi} - \frac{dx_j}{dt}\frac{d\hat{y}_i}{d\xi}} \left\langle \frac{dy_j}{dt}, -\frac{dx_j}{dt} \right\rangle. \tag{26}$$

The non-characteristic curves of (25) are obtained by one dimensional interpolation in between points lying on different characteristics, see the left illustration in Figure 4. The derivative u_ξ at the node where γ_j intersects ζ_i, is computed via the Lagrange polynomial interpolation along ζ_i.

In the particular case in which the characteristic curves are graphs, say $\left|\frac{dx_j}{dt}\right| > 0$, $j = 1,2,\ldots,m$, a different method is employed to compute the gradient: the first component of each characteristic is regarded as the independent variable x and the other components can be expressed as functions $y_j = \phi_j(x)$ and $\theta_j = \psi_j(x)$, $j = 1,2,\ldots,m$. Thus, letting $x^k = k\frac{c}{n-1}, k = 1,2,\ldots,n$ we approximate the value of the functions $\{y_j = \phi_j(x)\}_{j=1}^m$ and $\{\theta_j = \psi_j(x)\}_{j=1}^m$ at equally spaced points via fifth degree piecewise Lagrange polynomials. For simplicity, we denote the interpolated point of the j^{th} characteristic at x^k by (x^k, y_j^k, θ_j^k). We construct a curve $\zeta_k(\xi) = (\hat{x}_k(\xi), \hat{y}_k(\xi))$ as in

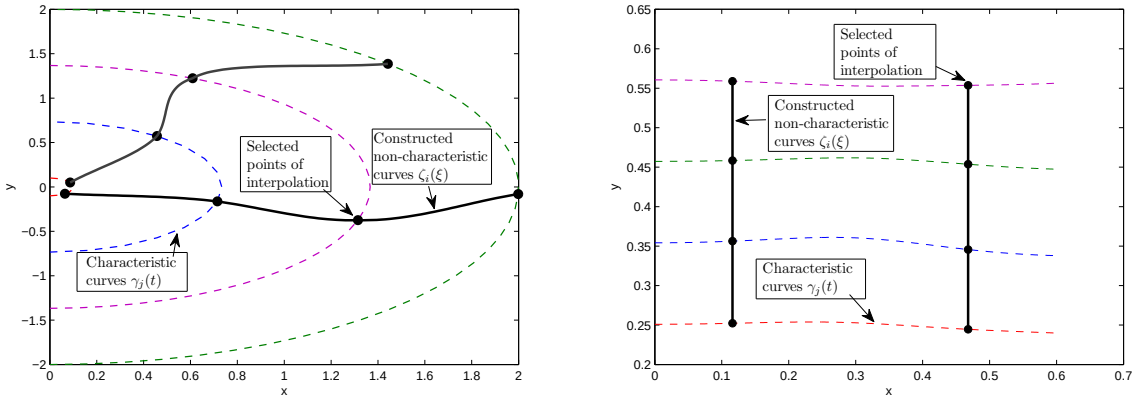

Figure 4. The left image illustrates an example of a set of constructed non-characteristic (solid line) curves as in (25) with selected points (solid dots) on the characteristic curves (dashed lines). The right image shows an example of a set of constructed non-characteristic curves (solid line) by selecting the points of interpolation (solid dots) on the characteristic curves (dashed lines) which can be described by functions. The reconstructed conductivities of the four modes and the brain, shown in Figure 5, were constructed on the characteristics computed as in step 1 of section 3.2 with non-characteristic and characteristic curves as in the the right image using (28).

(25) by fixing k and selecting $(x^k, y_j^k)_{j=1}^m$ as the points for interpolation (see the right illustration in Figure 4), so that $\frac{d\hat{x_k}}{d\xi} = 0$, $\frac{d\hat{y_k}}{d\xi} = 1$, and $u_\xi = u_y$. Using the first two equations in (11) and the curve ζ_k at the j^{th} point (x^k, y_j^k, θ_j^k), the formula (26) becomes

$$\nabla u = \frac{u_y}{\sin\theta_j^k} \left\langle \cos\theta_j^k, \sin\theta_j^k \right\rangle . \tag{27}$$

Note that since $y_j = \phi_j(x)$ for $j = 1, 2, \ldots, m$, then $0 < \theta < \pi$ for every $(x, \phi_j(x))$ in Ω, in particular $\sin\theta_j^k$ never vanishes.

Step 3. One recovers the conductivity by (26). In the specific case in which the equipotential curves are graphs the conductivity at (x^k, y_j^k) is also given by

$$\sigma(x^k, y_j^k) = \frac{|J|(x^k, y_j^k)}{u_y(x^k, y_j^k)} \sin\theta_j^k. \tag{28}$$

Note that in the case of graphs $u_y \neq 0$. The reconstructions in Figure 5 are done using formula (28).

The reconstruction method requires differentiation of the interior data, and the reconstructed potential. In the case of rough data, such as the brain experiment (see Figure 2), we use regularized differentiation, as explained below.

The interior data is convoluted with the two dimensional triangle function

$$T_{\epsilon_x,\epsilon_y}(x,y) = \begin{cases} \left(\frac{1-|x|}{\epsilon_x^2}\right) \cdot \left(\frac{1-|y|}{\epsilon_y^2}\right) & , \; if \; |x| \leq \epsilon_x \; and \; |y| \leq \epsilon_y \\ 0 & , \; otherwise \end{cases}$$

before differentiation by directional central difference. The reconstructed values of the potential are not available on a rectangular grid, which forces us to convolute u indirectly

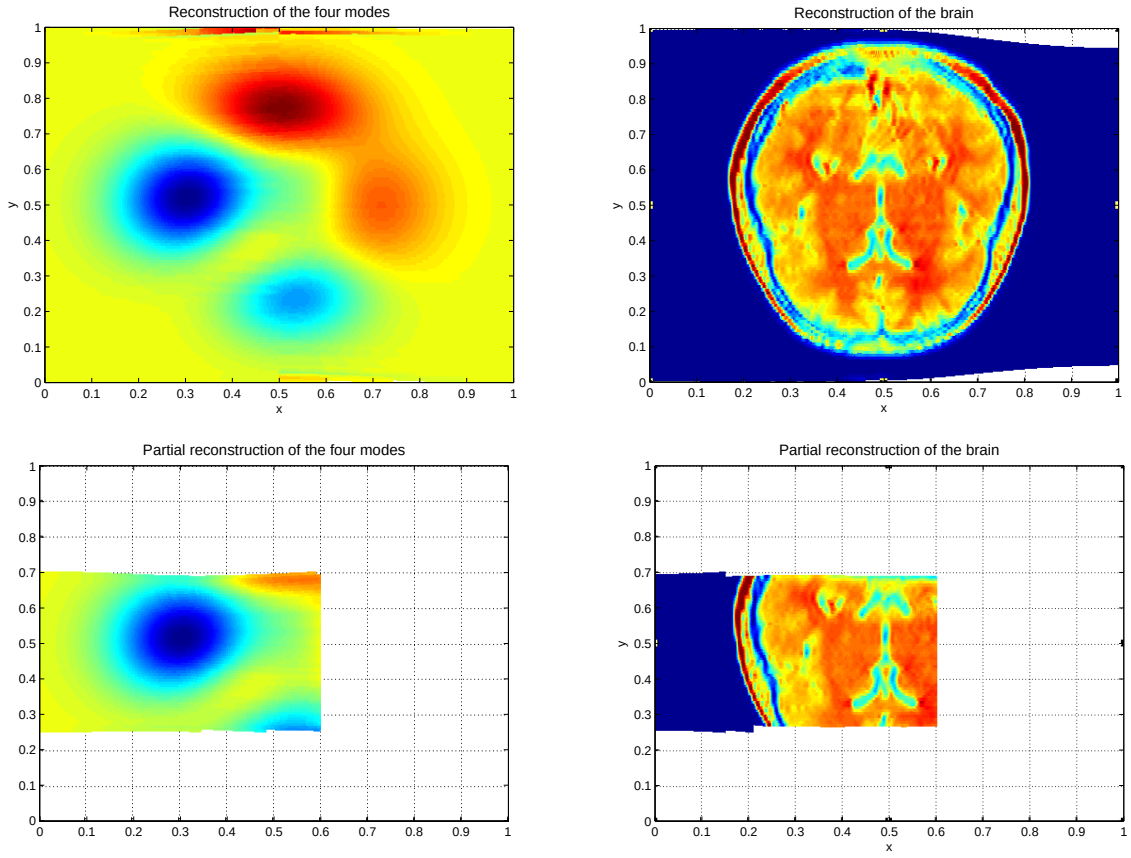

Figure 5. The top images show the reconstruction of the four modes (left) and the brain (right) reconstructed from the interior data measured in $[0,1]\times[0,1]$. The bottom images show the partial reconstruction of the four modes (left) and the brain (right) from the data measured in $[0,0.6]\times[0.25,0.701]$. The l_1 relative error for the reconstruction of the four modes and the brain from complete data are 0.18% and 1.37%, respectively.

by

$$\int_{-\infty}^{\infty}\int_{-\infty}^{\infty}\Phi(\alpha,\beta)T_{\epsilon_x,\epsilon_y}(u-\alpha,x-\beta)\mathrm{d}\alpha\mathrm{d}\beta,$$

where $x\mapsto(x,\Phi(u_0,x))$ is the parametrization of the equipotential curve with voltage potential u_0.

We stress that in this paper we only regularize the differentiation of the magnitude of the current density but not of the voltage potential generated numerically by solving (1). Moreover, in the case of smooth data, like in the four modes experiment, we did not use any regularization in the differentiation. The l_1-relative error

$$\frac{1}{mn}\sum_{j=1}^{m}\sum_{i=1}^{n}\frac{|\sigma-\tilde{\sigma}|}{\sigma}(x(t_{j_i}),y(t_{j_i}))$$

in the reconstruction of the brain from the complete interior data is 0.0137, and from incomplete interior data is 0.0149. The l_1-relative error of the reconstruction of the four

modes from the complete interior data is about 0.0018, and from incomplete data is 0.0028. See the Figure 5 for reconstructions from complete and incomplete data.

4. Concluding remarks

We presented a new planar conductivity reconstruction method in CDII based on solving the Cauchy problem for the 1-Laplacian with partial data. We show that equipotential lines are characteristics of a corresponding first order quasilinear PDE. In particular this emphasizes the specific (parabolic) character of the 1-Laplacian, namely that the solution on one side of the characteristic does not influence the solution on the other side. This fact was observed previously in [21], where the equipotential lines were shown to be geodesics in an appropriate Riemannian metric.

If $|J|$ is known in the entire domain Ω, then (by the uniqueness of solution in the initial value problem for ODEs,) the method recovers the entire equipotential line originating at Γ. From the weak maximum principle, in order for the characteristics to span the full domain it is necessary that

$$Range(f|_\Gamma) = Range(u|_{\partial\Omega}). \tag{29}$$

From the strong maximum principle, the maximum occurs on Γ_+ where the normally applied current is negative , while the minimum occurs on Γ_-, where the current is positive. Thus finding the maximum and minimum voltage entails measuring the potential on $\Gamma_\pm$. This is problematic in practice since $\Gamma_\pm$ are precisely where the electrodes are placed. However, if $\Gamma_\pm$ tend to a point (of injection), then the voltage on each of the two arcs of $\partial\Omega \setminus \Gamma\pm$ covers all of the voltage potential inside.

If, as considered in [21], instead of injecting a current, one maintains an almost two-to-one (i.e., each values is taken twice with the exception of the connected maxima and minima) boundary voltage and measures the exiting normal current at an arc Γ satisfying (29), then the method here also recovers the conductivity everywhere inside Ω.

Acknowledgments

The authors thank Guillaume Bal for the suggestion on the approach. This work was supported by NSF grant DMS-0905799.

References

[1] G. Alessandrini, *An identification problem for an elliptic equation in two variables*, Annali di matematica pura ed applicata, **145** (1986), pp. 265–295.

[2] G. Alessandrini and R. Magnanini, *The index of isolated critical points and solutions of elliptic equations in the plane*, Ann. Suola Norm. Sup. Pisa Cl. Sci. (4), **94** (1992), pp. 567–589.

[3] G. Alessandrini and R. Magnanini, *Elliptic equations in divergent form, geometric critical points of solutions, and Stekloff eigenfunctions*, SIAM J. Math. Anal., **35** (1994), pp. 1259–1268.

[4] H. Ammari, Y. Capdeboscq, H. Kang, and A. Kozhemiak, *Mathematical models and reconstruction methods in magneto-acouostic imaging*, European J. Appl. Math., **20**(2009), pp. 303–317.

[5] H. Ammari, E. Bonnetier, Y. Capdeboscq, M. Tanter, and M. Fink, *Electrical Impedance Tomography by Elastic Deformation*, SIAM J. Appl. Math., **68** (2008), pp.1557–1573.

[6] H. Ammari and H. Kang, *Multi-Scale and Multi-Physics Biomedical Imaging Modalities*, in Handbook of Mathematical Methods in Imaging, ed. O. Scherzer, Springer, New York, to appear.

[7] P. M. Anselon and P. J. Laurent, *A general method for construction of interpolating and smoothing spline-function*, Numer. Math., **12** (1968).

[8] L. Bers, F. John, and M. Schechter, *Partial Differential Equation*, John Wiley & Sons, New York, 1957.

[9] C. de Boor, *Bicubic spline interpolation*, J. Math. Phis., **41** (1962).

[10] B. Gebauer and O. Scherzer, *Impedance-acoustic tomography*, SIAM J. Appl. Math., **69** (2008), pp. 565–576.

[11] D. Gilbarg and N. S. Trudinger, *Elliptic Partial Differential Equations*, 2nd ed., Springer-Verlag, NY, 2001.

[12] M. W. Hirsh, C. C. Pugh, *Stable manifolds for hyperbolic sets*, Proc. Symp. Pure Math., **14**(1970), 133-163.

[13] M. J. Joy, A. I. Nachman, K. F. Hasanov, R. S. Yoon, and A. W. Ma, *A new approach to Current Density Impedance Imaging (CDII)*, Proceedings ISMRM, No. 356, Kyoto, Japan, 2004.

[14] S. Kim, O. Kwon, J. K. Seo, and J. R. Yoon, *On a nonlinear partial differential equation arising in magnetic resonance electrical impedance tomography*, SIAM J. Math. Anal., **34** (2002), pp. 511–526.

[15] O. Kwon, E. J. Woo, J. R. Yoon, and J. K. Seo, *Magnetic resonance electric impedance tomography (MREIT): Simulation study of J-substitution algorithm*, IEEE Trans. Biomed. Eng., **49** (2002), pp. 160–167

[16] O. Kwon, J. Y Lee, and J. R. Yoon, *Equipotential line method for magnetic resonance electrical impedance tomography*, Inverse Problems. **18** (2002), pp. 1089-1100

[17] J. Y. Lee *A reconstruction formula and uniqueness of conductivity in MREIT using two internal current distributions*, Inverse Problems, **20** (2004), pp. 847–858

[18] J. J. Liu, J. K. Seo, M. Sini and E. J. Woo, *On the conductivity imaging by MREIT: available resolution and noisy effect*, J. Phys.: Conf. Ser. **73** (2007), 012015 (20pp).

[19] J. J. Liu, J. K. Seo, M. Sini and E. J. Woo, *On the convergence of the harmonic Bz Algorithm in Magnetic Resonance Imaging*, SIAM J. Appl. Math. **67** (2007), 1259–1282.

[20] Q. Ma and B. He, *Investigation on magnetoacoustic signal generation with magnetic induction and application to electrical conductivity reconstruction*, Phys. Med. Biol., **52** (2007), pp. 5085–5099.

[21] A. Nachman, A. Tamasan, and A. Timonov, *Conductivity imaging with a single measurement of boundary and interior data*, Inverse Problems, **23** (2007), pp. 2551–2563.

[22] A. Nachman, A. Tamasan, and A. Timonov, *Recovering the conductivity from a single measurement of interior data*, Inverse Problems, **25** (2009) 035014 (16pp).

[23] A. Nachman, A. Tamasan, and A. Timonov, *Reconstruction of planar conductivities in subdomains from incomplete data*, SIAM J. Appl. Math., **70**(2010), 3342 –3362.

[24] A. Nachman, A. Tamasan, and A. Timonov, *Current Density Impedance Imaging*, preprint.

[25] M. Z. Nashed and A. Tamasan, *Structural stability in a minimization problem and applications to conductivity imaging*, Inverse Probl. Imaging, **5** (2010), 219–236.

[26] G. C. Scott, M. L. Joy, R. L. Armstrong, and R. M. Henkelman, *Measurement of nonuniform current density by magnetic resonance*, IEEE Trans. Med. Imag., **10** (1991), pp. 362–374

[27] E. J. Woo and J. K. Seo, *Magnetic resonance electrical impedance tomography (MREIT) for*

high resolution conductivity imaging, Physiol. Meas., **29** (2008), pp. R1-R26.

[28] X. Li, Y. Xu and B. He, *Imaging Electrical Impedance from Acoustic Measurements by Means of Magnetoacoustic Tomography with Magnetic Induction (MAT-MI)*, IEEE Transactions on Biomedical Engineering, 54(2007), pp. 323330.

[29] N. Zhang, *Electrical impedance tomography based on current density imaging*, Thesis: University of Toronto, Canada, 1992.